

## A polymer electrolyte with high luminous transmittance and low solar throughput: Polyethyleneimine-lithium bis(trifluoromethylsulfonyl) imide with In<sub>2</sub>O<sub>3</sub>:Sn nanocrystals

İ. Bayrak Pehlivan, E. L. Runnerstrom, S.-Y. Li, G. A. Niklasson, D. J. Milliron et al.

Citation: *Appl. Phys. Lett.* **100**, 241902 (2012); doi: 10.1063/1.4728994

View online: <http://dx.doi.org/10.1063/1.4728994>

View Table of Contents: <http://apl.aip.org/resource/1/APPLAB/v100/i24>

Published by the [American Institute of Physics](http://www.aip.org).

---

### Related Articles

Structural variation of hydrothermally synthesized KNbO<sub>3</sub> nanowires  
*J. Appl. Phys.* **111**, 114314 (2012)

Long lifetime, high density single-crystal erbium compound nanowires as a high optical gain material  
*Appl. Phys. Lett.* **100**, 241905 (2012)

A new type of optical biosensor from DNA wrapped semiconductor graphene ribbons  
*J. Appl. Phys.* **111**, 114703 (2012)

Nanomanipulation and nanofabrication with multi-probe scanning tunneling microscope: From individual atoms to nanowires  
*Rev. Sci. Instrum.* **83**, 063704 (2012)

Electrical growth of metallic nanoparticles in mesoporous silica films using atomic force microscopy  
*Appl. Phys. Lett.* **100**, 241605 (2012)

---

### Additional information on *Appl. Phys. Lett.*

Journal Homepage: <http://apl.aip.org/>

Journal Information: [http://apl.aip.org/about/about\\_the\\_journal](http://apl.aip.org/about/about_the_journal)

Top downloads: [http://apl.aip.org/features/most\\_downloaded](http://apl.aip.org/features/most_downloaded)

Information for Authors: <http://apl.aip.org/authors>

## ADVERTISEMENT

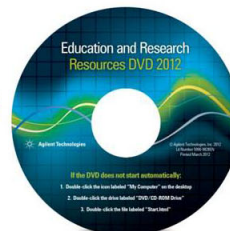


**Agilent Technologies**

### Agilent Education and Research Resources DVD 2012

Packed with over **100 NEW** articles, application notes, webcasts, and videos relating to Renewable Energy, Nanoscience, RF/Wireless, MIMO, Materials, Digital Signals, Photonics, and General Test & Measurement.

Click Here to  
Order Your DVD



Agilent Technologies

## A polymer electrolyte with high luminous transmittance and low solar throughput: Polyethyleneimine-lithium bis(trifluoromethylsulfonyl) imide with $\text{In}_2\text{O}_3:\text{Sn}$ nanocrystals

İ. Bayrak Pehlivan,<sup>1,a)</sup> E. L. Runnerstrom,<sup>2,3</sup> S.-Y. Li,<sup>1</sup> G. A. Niklasson,<sup>1</sup> D. J. Milliron,<sup>2</sup> and C. G. Granqvist<sup>1</sup>

<sup>1</sup>Department of Engineering Sciences, The Ångström Laboratory, Uppsala University, P. O. Box 534, SE-75121 Uppsala, Sweden

<sup>2</sup>The Molecular Foundry, Lawrence Berkeley National Laboratory, Berkeley, California 94720, USA

<sup>3</sup>Department of Materials Science and Engineering, University of California, Berkeley, California 94720, USA

(Received 22 February 2012; accepted 25 May 2012; published online 14 June 2012)

Chemically prepared  $\sim 13$ -nm-diameter nanocrystals of  $\text{In}_2\text{O}_3:\text{Sn}$  were included in a polyethyleneimine-lithium bis(trifluoromethylsulfonyl) imide electrolyte and yielded high haze-free luminous transmittance and strong near-infrared absorption without deteriorated ionic conductivity. The optical properties could be reconciled with effective medium theory, representing the  $\text{In}_2\text{O}_3:\text{Sn}$  as a free electron plasma with tin ions screened according to the random phase approximation corrected for electron exchange. This type of polymer electrolyte is of large interest for opto-ionic devices such as laminated electrochromic smart windows. © 2012 American Institute of Physics. [<http://dx.doi.org/10.1063/1.4728994>]

This Letter introduces a polymer electrolyte based on polyethyleneimine and lithium bis(trifluoromethylsulfonyl) imide (PEI-LiTFSI) and containing nanocrystals of tin-doped indium oxide (i.e.,  $\text{In}_2\text{O}_3:\text{Sn}$  or ITO). This electrolyte combines high luminous transmittance  $T_{\text{lum}}$  with low solar transmittance  $T_{\text{sol}}$  and is of much interest for opto-ionic devices such as laminated electrochromic smart windows for energy efficient buildings.<sup>1-3</sup>

Electrochromic smart windows typically comprise a multilayer structure with a centrally positioned electrolyte usually being an inorganic thin film or a polymer electrolyte layer.<sup>4</sup> The latter option allows long open-circuit memory and uniform color changes and is also preferable for manufacturing.<sup>3</sup> Our prior work considered a PEI-LiTFSI model electrolyte and embraced ion relaxation mechanisms,<sup>5,6</sup> mechanical properties,<sup>7</sup> and  $\text{SiO}_2$  nanoparticles to boost the ionic conductivity without sacrificing optical performance.<sup>8</sup>

In some applications of smart windows, it is preferable to minimize the near-infrared solar transmittance (in the  $700 < \lambda < 3000$  nm wavelength range) irrespectively of  $T_{\text{lum}}$  (at  $400 < \lambda < 700$  nm). As shown here, this functionality can be obtained by dispersing ITO nanocrystals in a PEI-LiTFSI electrolyte. ITO is a transparent conductor; the  $\text{In}_2\text{O}_3$  semiconductor host has a wide band gap, and substitutional doping of Sn atoms on In sites yields free electrons whose density can be sufficient for plasmon absorption in the near-infrared.<sup>9,10</sup>

PEI-LiTFSI was prepared by mixing branched PEI (molecular weight 10 000) and  $\text{LiN}(\text{CF}_3\text{SO}_2)_2$  in methanol and proceeding as previously described.<sup>5</sup> The PEI:LiTFSI molar ratio—defined as the number of moles of the PEI repeating units,  $-(\text{CH}_2\text{CH}_2\text{NH})-$ , divided by the number of moles of LiTFSI—was 50:1, which yields maximum ionic conductivity.<sup>6</sup> ITO nanocrystals with an Sn/In ratio of 5 at. % were prepared by standard Schlenk-line techniques

as reported elsewhere,<sup>11</sup> and their oleylamine and oleic acid ligands were stripped using  $\text{NOBF}_4$ .<sup>12,13</sup> The resulting bare, hydrophilic nanocrystals were stabilized by  $\text{BF}_4^-$  anions in a dimethylformamide (DMF) solution. Finally, known quantities of PEI-LiTFSI and ITO-DMF solutions were mixed and kept at  $65^\circ\text{C}$  and  $10^{-1}$  mbar for 48 h to remove methanol and DMF. Nanocomposite electrolytes of (PEI-ITO)-LiTFSI were made with up to 7 wt. % of ITO (counted as a fraction of the total weight of ITO and PEI). The transmission electron microscope (TEM) image in Fig. 1 shows colloidal ITO nanocrystals, prior to ligand exchange, with diameters  $D$  of  $13 \pm 3$  nm; high-resolution TEM and x-ray diffraction (not shown) indicated that the nanocrystals are highly crystalline with the  $\text{In}_2\text{O}_3$  bixbyite phase. Figure 1 also reports an absorbance spectrum for such colloidal ITO nanocrystals and demonstrates a strong absorption peak at  $\lambda \approx 1830$  nm.

Temperature dependent ionic conductivity  $\sigma(\tau)$  was recorded by impedance spectroscopy in the frequency range of  $10^{-1}$  to  $10^7$  Hz for  $23 < \tau < 70^\circ\text{C}$  as described elsewhere.<sup>5-8</sup> Figure 2 reports  $\sigma$  at six temperatures for samples with 0, 1, 3, 5, and 7 wt. % ITO and shows that  $\sigma$  is rather independent of the ITO content and rises monotonically from  $\sim 1 \times 10^{-6}$  S/cm at  $23^\circ\text{C}$  to  $\sim 2 \times 10^{-5}$  at  $70^\circ\text{C}$ ;  $\sigma(\tau)$  obeys an Arrhenius behavior with activation energy of  $\sim 52.5$  kJ/mol.

Spectral total and diffuse transmittance and reflectance were measured at  $300 < \lambda < 2500$  nm for (PEI-ITO)-LiTFSI layers sandwiched between microscope glass slides using a metal foil as a spacer; the layer thickness was  $70 \pm 10$   $\mu\text{m}$  as determined mechanically. The diffuse components in the optical spectra were  $< 1\%$  in transmittance and  $< 0.3\%$  in reflectance and hence negligible. Solid curves in Fig. 3 show spectral transmittance. Without ITO, the transmittance is large for  $\lambda < 1500$  nm while there are absorption bands due to PEI at  $\lambda > 1500$  nm. When ITO is added, the transmittance remains high in the luminous range but decreases sharply in the near-infrared. Reflectance (not shown) was 7 to 8% in the luminous range and  $\sim 4\%$  in the near-infrared. Hence, the

<sup>a)</sup>Electronic mail: [ilknur.pehlivan@angstrom.uu.se](mailto:ilknur.pehlivan@angstrom.uu.se).

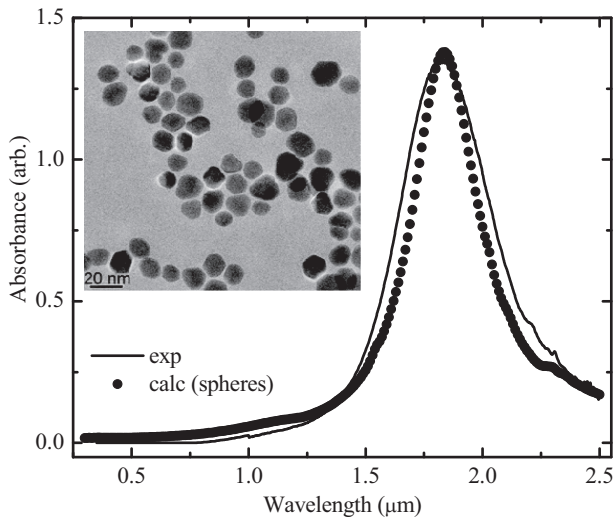


FIG. 1. Main figure shows spectral absorbance as measured using an ASD Quality Spec Pro VIS/NIR spectrometer for an as-synthesized (non-ligand exchanged) dilute suspension of colloidal ITO nanocrystals (solid curve) and as computed from a model described in the main text (symbols; the vertical scale was adjusted to coincide with the measurement at the peak). Inset depicts a TEM image of ITO nanocrystals; data were obtained with a JEOL 2100 operated at 200 kV.

low transmittance in Fig. 3 is caused by an absorption band whose intensity depends on the ITO content. Table I shows  $T_{lum}$  and  $T_{sol}$  obtained from

$$T_{lum,sol} = \int d\lambda \varphi_{lum,sol}(\lambda) T(\lambda) / \int d\lambda \varphi_{lum,sol}(\lambda), \quad (1)$$

where  $\varphi_{lum}$  is the sensitivity of the light-adapted human eye<sup>14</sup> and  $\varphi_{sol}$  is solar irradiance for air mass 1.5 (the sun at 37° above the horizon).<sup>15</sup>

The optical data in Fig. 3 are theoretically addressed next. We assume that ITO nanoparticles with  $D \ll \lambda$  are em-

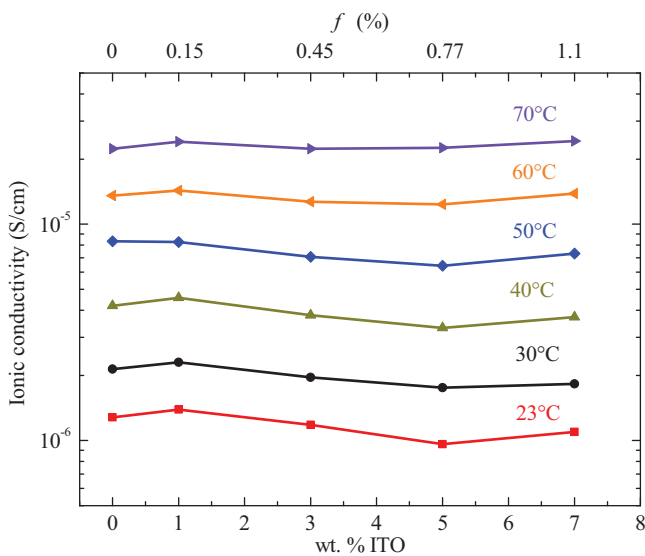


FIG. 2. Ionic conductivity vs ITO content in wt. % as well as volume fraction (filling factor,  $f$ ) at the shown temperatures. Data points are indicated by symbols, which are joined by straight lines for convenience. The data were taken by use of a Novocontrol BDC-N dielectric interface together with a Solartron 1260 frequency analyzer; the applied ac voltage was 1 V.

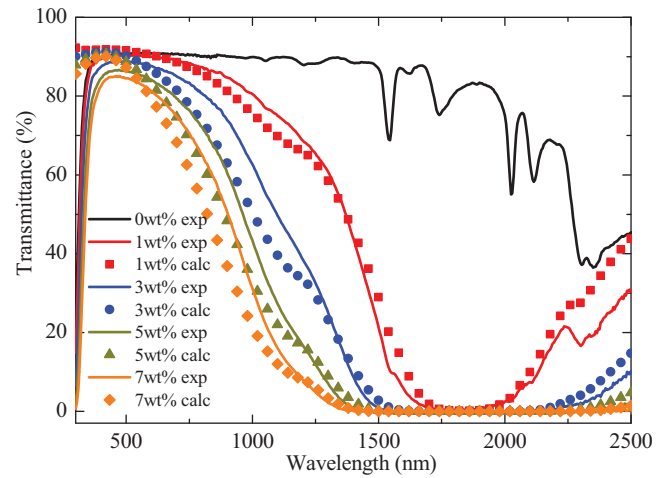


FIG. 3. Spectral transmittance for the shown ITO contents as measured (solid curves) and calculated (symbols) for  $\sim 70$ - $\mu$ m-thick (PEI-ITO)-LiTFSI. The measurement used a Perkin Elmer 900 spectrophotometer with a barium-sulphate-coated integrating sphere. The sharp drops at the shortest wavelengths are dominated by absorption in the glass slides.

bedded in a continuous matrix, which implies that a Maxwell-Garnett effective medium treatment is appropriate.<sup>16,17</sup> Following established notation,<sup>18–20</sup> the effective dielectric function  $\epsilon^{MG}$  is

$$\epsilon^{MG} = \epsilon_m (1 + \frac{2}{3} f \alpha) / (1 - \frac{1}{3} f \alpha), \quad (2)$$

where  $\epsilon_m$  is the dielectric permeability for the matrix and  $f$  is the “filling factor,” i.e., the particles’ volume fraction. For reasons given below, we consider a random distribution of ellipsoidal particles so that

$$\alpha = \frac{1}{3} \sum_{i=1}^3 \frac{\epsilon_p - \epsilon_m}{\epsilon_m + L_i (\epsilon_p - \epsilon_m)}, \quad (3)$$

where  $\epsilon_p$  is the dielectric function of the nanocrystals and the  $L_i$ s are a triplet of depolarization factors given by the nanocrystals’ shape. Spheres have  $L_i = 1/3$ . Refinements of the theoretical model encapsulated in Eqs. (2) and (3) are possible.<sup>21</sup>

Our calculations assumed ITO nanocrystals in a polymer host, and  $f$  was calculated from weight percentages. We obtained  $\epsilon_m$  from handbook values of the refractive index together with spectrophotometric measurements of the absorption coefficient.<sup>22</sup> The nanocrystal dielectric function  $\epsilon_p$  was taken as  $\epsilon_{ITO}$  and was computed as in earlier work,<sup>9</sup> assuming a free electron plasma with singly charged tin impurities screened according to the random phase approximation with exchange represented by Hubbard’s model.<sup>23</sup>

TABLE I. Luminous and solar transmittance,  $T_{lum}$  and  $T_{sol}$ , for  $\sim 70$ - $\mu$ m-thick (PEI-ITO)-LiTFSI layers with different ITO content.

ITO content (wt. %)	0	1	3	5	7
$T_{lum}$ (%)	91.7	90.7	88.7	85.7	83.3
$T_{sol}$ (%)	88.9	77.3	68.8	61.1	56.3

We first modeled the absorbance data in Fig. 1 using a free electron density  $n_e$  of  $9.8 \times 10^{20} \text{ cm}^{-3}$ ,<sup>24</sup> and this value was then employed to represent the data in Fig. 3. It is seen that theory and experiment are in good semi-quantitative agreement for all samples. The calculated data display a weak “shoulder” at  $\lambda \approx 1200 \text{ nm}$ ; its origin is unknown, but it is striking that this feature lies close to a wavelength where the real part of ITO’s dielectric function crosses zero and the real part of the corresponding dynamic resistivity has a “knee.”<sup>9</sup> Some other minor discrepancies can also be found between experimental and theoretical data, and nanocrystal aggregation deserves consideration as a possible source of those. Dipole-dipole interaction due to clustering can be included in an effective medium treatment via *effective* depolarization factors, denoted  $L_i^*$ , in Eq. (3). Specifically aggregates in the form of chains and fcc clusters are represented by triplets of  $L_i^*$ s being (0.133, 0.435, 0.435) and (0.0865, 0.0865, 0.827), respectively.<sup>25</sup> Figure 4 illustrates the effect of including aggregates in the model for a sample with 1 wt. % ITO and again using  $n_e = 9.8 \times 10^{20} \text{ cm}^{-3}$ . In this case, the model clearly diverges, which lends additional credence to our conclusion that the optical data in Fig. 3 are consistent with essentially well-dispersed ITO nanocrystals. Non-spherical shapes of the ITO nanocrystals, evident from Fig. 1, may add some broadening of the transmittance minimum in Fig. 3, though.<sup>26</sup>

In summary, we have incorporated ITO nanocrystals in a transparent polymer electrolyte and demonstrated that high haze-free luminous transmittance can be combined with strong near-infrared absorption without compromising ionic conductivity. An effective medium treatment for well-separated nanocrystals could be reconciled with the optical data. Our material is of large interest for opto-ionic devices such as laminated electrochromic smart windows. We note that our work is a proof-of-principle, and there are innumerable ways for development by using alternative polymer electrolyte hosts<sup>27</sup> and other kinds of transparent conducting nanoparticles such as ZnO:Al,<sup>28</sup> SnO<sub>2</sub>:Sb,<sup>29</sup> M<sub>x</sub>WO<sub>3</sub> (M being Na, K, or Cs),<sup>30,31</sup> or LaB<sub>6</sub>.<sup>32,33</sup> There are also numerous routes to nanoparticle and

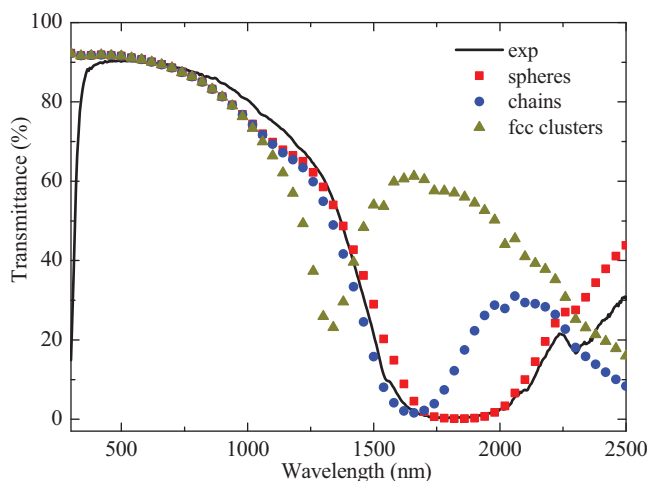


FIG. 4. Spectral transmittance for  $\sim 70\text{-}\mu\text{m}$ -thick (PEI-ITO)-LiTFSI with 1 wt. % ITO as measured (solid curve, also shown in Fig. 3) and computed (symbols) using (effective) depolarization factors appropriate to spheres, chains, and fcc clusters.

nanowire fabrication, as recently surveyed for ITO.<sup>34</sup> An interesting development of the present work would be to use VO<sub>2</sub>-based nanoparticles<sup>20</sup> to enable devices with joint electro- and thermochromism.

Research at Uppsala University was supported by the Swedish Research Council (VR) and the Swedish Research Council for Environment, Agricultural Sciences, and Spatial Planning (FORMAS). İBP acknowledges a travel grant from Anna-Maria Lundin’s Foundation at *Natio Smolandica*. Research at the Molecular Foundry was supported by the U.S. Department of Energy, including an Early Career Research Program grant to DJM, under Contract No. DE-AC02-05CH11231, and by the UC Berkeley Chancellor’s Fellowship for Graduate Study to ELR. We acknowledge Dr. Raffaella Buonsanti for TEM characterization and helpful discussions.

- <sup>1</sup>G. A. Niklasson and C. G. Granqvist, *J. Mater. Chem.* **17**, 127 (2007).
- <sup>2</sup>G. B. Smith and C. G. Granqvist, *Green Nanotechnology: Solutions for Sustainability and Energy in the Built Environment* (CRC, Boca Raton, FL, 2010).
- <sup>3</sup>C. G. Granqvist, *Sol. Energy Mater. Sol. Cells* **99**, 1 (2012).
- <sup>4</sup>C. G. Granqvist, *Handbook of Inorganic Electrochromic Materials* (Elsevier, Amsterdam, The Netherlands, 1995).
- <sup>5</sup>İ. Bayrak Pehlivan, R. Marsal, P. Georén, C. G. Granqvist, and G. A. Niklasson, *J. Appl. Phys.* **108**, 074102 (2010).
- <sup>6</sup>İ. Bayrak Pehlivan, P. Georén, R. Marsal, C. G. Granqvist, and G. A. Niklasson, *Electrochim. Acta* **57**, 201 (2011).
- <sup>7</sup>İ. Bayrak Pehlivan, R. Marsal, C. G. Granqvist, G. A. Niklasson, and P. Georén, *Sol. Energy Mater. Sol. Cells* **94**, 2399 (2010).
- <sup>8</sup>İ. Bayrak Pehlivan, C. G. Granqvist, R. Marsal, P. Georén, and G. A. Niklasson, *Sol. Energy Mater. Sol. Cells* **98**, 465 (2012).
- <sup>9</sup>I. Hamberg and C. G. Granqvist, *J. Appl. Phys.* **59**, 2950 (1986); **60**, R123 (1986).
- <sup>10</sup>Recently, compositional tuning of the near-infrared plasmon absorption was demonstrated for solvent-dispersed ITO nanocrystals synthesized by organic phase colloidal methods; cf. M. Kanehara, H. Koike, T. Yoshinaga, and T. Teranishi, *J. Am. Chem. Soc.* **131**, 17736 (2009) and G. Garcia, R. Buonsanti, E. L. Runnerstrom, R. J. Mendelsberg, A. Llordes, A. Anders, T. J. Richardson, and D. J. Milliron, *Nano Lett.* **11**, 4415 (2011).
- <sup>11</sup>S.-I. Choi, K. M. Nam, B. K. Park, W. S. Seo, and J. T. Park, *Chem. Mater.* **20**, 2609 (2008).
- <sup>12</sup>A. Dong, X. Ye, J. Chen, Y. Kang, T. Gordon, J. M. Kikkawa, and C. B. Murray, *J. Am. Chem. Soc.* **133**, 998 (2011).
- <sup>13</sup>A. Llordes, A. T. Hammack, R. Buonsanti, R. Tangirala, S. Aloni, B. A. Helms, and D. J. Milliron, *J. Mater. Chem.* **21**, 11631 (2011).
- <sup>14</sup>G. Wyszecki and W. S. Stiles, *Color Science: Concepts and Methods, Quantitative Data and Formulae*, 2nd ed. (Wiley, New York, 2000).
- <sup>15</sup>ASTM G173-03 Standard Tables of Reference Solar Spectral Irradiances: Direct Normal and Hemispherical on a 37° Tilted Surface, *Annual Book of ASTM Standards* (American Society for Testing and Materials, Philadelphia, PA, 2008), Vol. 14.04; <http://rredc.nrel.gov/solar/spectra/am1.5>.
- <sup>16</sup>J. C. Maxwell-Garnett, *Philos. Trans. R. Soc. London, Ser. A* **203**, 385 (1904); **205**, 237 (1906).
- <sup>17</sup>G. A. Niklasson, C. G. Granqvist, and O. Hunderi, *Appl. Opt.* **20**, 26 (1981).
- <sup>18</sup>C. G. Granqvist and O. Hunderi, *Phys. Rev. B* **16**, 3513 (1977).
- <sup>19</sup>C. G. Granqvist and O. Hunderi, *Phys. Rev. B* **18**, 2897 (1978).
- <sup>20</sup>S.-Y. Li, G. A. Niklasson, and C. G. Granqvist, *J. Appl. Phys.* **108**, 063525 (2010).
- <sup>21</sup>D. Dalacu and L. Martinu, *J. Vac. Sci. Technol. A* **17**, 877 (1999).
- <sup>22</sup>Refractive index was taken from published data for PEI [T. M. Madkour, in *Polymer Data Handbook*, edited by J. E. Mark (Oxford University Press, Oxford, UK, 1999), pp. 490–492]; absorption coefficient was determined from the ratio of the transmittance of the polymer between the glass slides to the transmittance of the bare glass slides without spacer.
- <sup>23</sup>The random phase approximation [J. Lindhard, *Kgl. Danske Videnskab. Selskab Mat.-Fys. Medd.* **28**(8) (1954)] was corrected for exchange [J. Hubbard, *Proc. R. Soc. London, Ser. A* **243**, 336 (1957)]; further improvement to include correlation [K. S. Singwi, M. P. Tosi, R. H. Land, and A. Sjölander, *Phys. Rev.* **176**, 589 (1968)] is possible but is not expected to

be significant. In principle,  $\epsilon_{\text{ITO}}$  should be corrected for a limited mean free path  $\ell$  of the free electrons caused by the small particle size [U. Kreibig and M. Vollmer, *Optical Properties of Metal Clusters* (Springer, Berlin, Germany, 1995)], but this effect is believed to be minor since  $\ell$  is as short as  $\sim 5$  nm in the infrared (though increasing progressively towards shorter wavelengths since screening of the tin ions then becomes less efficient).

<sup>24</sup>Electron densities up to  $2.5 \times 10^{21} \text{ cm}^{-3}$  have been observed several times for ITO films; cf. C. G. Granqvist, *Sol. Energy Mater. Sol. Cells* **91**, 1529 (2007).

<sup>25</sup>P. Clippe, R. Evrard, and A. A. Lucas, *Phys. Rev. B* **14**, 1715 (1976). Their approach relied on detailed calculations on the resonance frequencies for several geometrically well-defined entities comprised of identical spheres such as pairs, infinite single- and double strand chains, and a close-packed fcc lattice. It was used in earlier work on gas evaporated gold (Ref. 18), which is a three-dimensional composite of metal and air. In principle, higher order multipole effects might be needed in a more complete analysis [A. Pack, M. Hietschold, and R. Wannemacher, *Opt. Commun.* **194**, 277 (2001)], but their effect is small since our ITO nanocrystals are separated from each other as inferred from recent work on samples similar to those studied in this Letter [R. J. Mengelsberg, G. Garcia, and D. J. Milliron, *J. Appl. Phys.* **111**, 063515 (2012)].

<sup>26</sup>Polyhedral shapes can be accounted for; cf. D. Langbein, *J. Phys. A: Math. Gen.* **10**, 1031 (1977); A. V. Goncharenko, V. Z. Lozovski, and E. F. Venger, *J. Phys.: Condens. Matter* **13**, 8217 (2001).

<sup>27</sup>*Polymer Electrolytes: Fundamentals and Applications*, edited by C. Sequeira and D. Santos (Woodhead, Sawston, UK, 2010).

<sup>28</sup>R. Buonsanti, A. Llordes, S. Aloni, B. A. Helms, and D. J. Milliron, *Nano Lett.* **11**, 4706 (2011).

<sup>29</sup>T. G. Conti, A. J. Chiquito, R. A. da Silva, E. Longo, and E. R. Leite, *J. Am. Ceram. Soc.* **93**, 3862 (2010).

<sup>30</sup>C. Guo, S. Yin, M. Yan, and T. Sato, *J. Mater. Chem.* **21**, 5099 (2011); C. Guo, S. Yin, L. Huang, L. Yang, and T. Sato, *Chem. Commun.* **47**, 8853 (2011).

<sup>31</sup>M. Mamak, S. Y. Choi, U. Stadler, R. Dolbec, M. Boulos, and S. Petrov, *J. Mater. Chem.* **20**, 9855 (2010).

<sup>32</sup>S. Schelm and G. B. Smith, *Appl. Phys. Lett.* **82**, 4346 (2003); S. Schelm, G. B. Smith, P. D. Garrett, and W. K. Fisher, *J. Appl. Phys.* **97**, 124314 (2005).

<sup>33</sup>H. Takeda, H. Kuno, and K. Adachi, *J. Am. Ceram. Soc.* **91**, 2897 (2008); K. Adachi, M. Miratsu, and T. Asahi, *J. Mater. Res.* **25**, 510 (2010).

<sup>34</sup>E. N. Dattoli and W. Lu, *MRS Bull.* **36**, 782 (2011).